Relation between graphitization of organic matter and clay mineralogy, Silurian black shales in Central Spain

J. F. Barrenechea, M. Rodas

Departamento de Cristalografía y Mineralogía, Facultad de Geología, U.C.M., 28040 Madrid, Spain

AND

A. Arche

Instituto de Geología Económica, C.S.I.C.-U.C.M., Facultad de Geología, 28040 Madrid, Spain

Abstract

A horizon containing graphite in the Early Silurian slates of the Eastern Central System, Central Spain, has been studied. The carbonaceous slates contain quartz, muscovite, graphitized organic matter, plagioclase, pyrite and apatite; and the slates above the graphite horizon contain quartz, phengite, plagioclase and chlorite. The origin of the graphite is related to a period of very slow accumulation rate, anoxic seafloors, deep-water upwellings and plankton blooms. The chlorite and graphite are mutually exclusive and by using the chlorite Al^{IV} content and the graphite c_o parameter, the conditions of metamorphism were calculated to be 300 ± 20 °C and 1.5–2 kbar.

Keywords: graphite, Early Silurian, Spanish Central System, anchi-epimetamorphism, chlorite, illite crystallinity.

Introduction

This paper deals with a reconstruction of the metamorphic conditions during the Hercynian deformation in an area of the Central System–the Serracin Syncline–using the physico-chemical characteristics of the graphitized organic matter and the phyllosilicates of the slates.

Recent literature on organic matter associated with low and very low grade metamorphic rocks shows successive stages in the evolution of carbonaceous matter to graphite. Many authors have observed changes in the crystallinity, elemental composition and physical properties of the carbonaceous matter related to diagenesis and progressive metamorphism (French, 1964; Griffin, 1967; Landis, 1971; Diessel and Offler, 1975). The general process is called graphitization, although Diessel *et al.* (1978) and Teichmüller (1987) restrict the use of the term to the most advanced stages, and call coalification the initial, low-grade stages. The evolution of organic matter depends on temperature and, to a lesser degree, on the period of heating (Castaño and Sparks, 1974). According to Shengelia *et al.* (1979), the graphite c_o parameter decreases with increasing temperature. As pressure and retrometamorphism do not affect substantially the c_o parameter, graphite may be used as a reliable geothermometer.

The passage from diagenesis to low-grade metamorphism was determined from the phyllosilicate mineralogy in the sandy slates above and below the horizon with graphitized organic matter, according to transformations described by Kubler (1967), Velde (1965) and Kisch (1980).

The Al^{IV} content of the chlorites has been used to determine their formation temperature using relations proposed by Cathelineau and Nieva (1985) and Cathelineau (1988).

Geological background

The graphite mineralization studied here is located in an area south of El Muyo, Segovia Province, in the eastern part of the Spanish Central System as defined by Bellido *et al.* (1981). The Ordovician and Silurian quartzites and slates

form a wide syncline, the Serracin Syncline, trending N–S (Fig. 1). The geology of the area has been reviewed in detail by González Lodeiro (1983).

From the base upwards, the following sequence has been established:

Rodada Slates (Schäfer, 1969): slates and some thin quartzites of Middle–Late Ordovician age.

Santibañez Quartzites (Schäfer, 1969): quartzites in thick banks of Basal Silurian (Llandovery) age.

Cañamares Slates (Bultynck and Soers, 1971) equivalent to the Serracin Slates (Bischoff, 1974): subdivided into a lower unit, 20 m thick, containing graphite and an upper unit, 80–100 m thick, of slates and thin quartzites of Lower to Upper Silurian (Llandovery–Basal Ludlow) age.

Successive Hercynian deformation phases are represented in the area, especially F_1, with tight folds with an almost vertical axial plane, and F_3 with axial planar folds dipping to the E. Both structures interfere in a type 3 superposition of Ramsay (González Lodeiro, 1983). A late, fourth phase creates NNE–SSW folds and the Hercynian deformation ends with a late wrench faulting phase.

According to Fuster *et al.* (1974), low-grade regional metamorphism was prevalent in the Eastern Central System, with a facies progressive series similar to the Barrovian model: great depth and low temperature gradient, achieving a maximum between the first and the second deformation phases. The typical mineralogy in the Silurian slates is: quartz + chlorite + muscovite ± albite ± pyrophyllite ± allevardite ± kaolinite ± chloritoid (Aparicio and Galán, 1980).

Sedimentological background. The sediments considered contain a rich marine fauna (graptolites, conchostraceae) and trace fossils. The Santibañez Quartzite presents large-scale, unidirectional trough cross-stratification and many internal scars. The geometry of the sandstone bodies is visible in the study area as large megaripples some metres high. They are interpreted as high-energy sand bodies dominated by wave and tide action on a continental shelf, comparable to contemporary examples from the North Sea (Stride, 1982) or South Africa (Martin and Fleming, 1986).

The lower part of the Serracin Slates is very different, with fine-grained, dark slates with parallel lamination, high organic carbon content and absence of bioturbation. The accumulation rate was very small, about 2.8–4 m per million

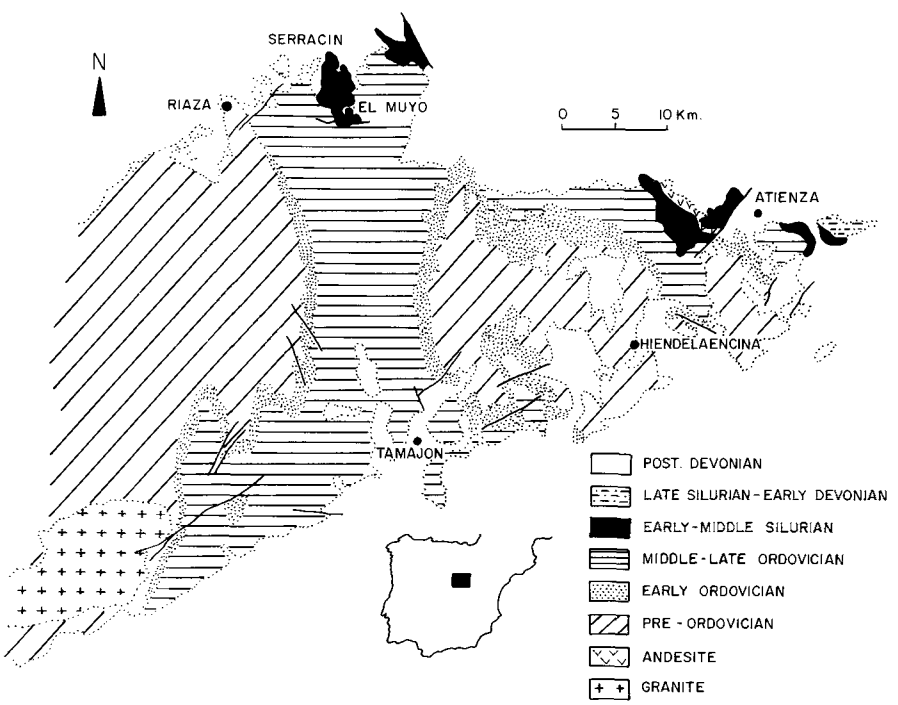

FIG. 1. Geological map of the Eastern Central System (after Soers, 1972).

years, determined from the stratigraphic control provided by graptolites found in these levels. They are interpreted as low-energy sediments deposited below wave action in the outer parts of the continental shelf (Hallam and Bradshaw, 1979; Legget 1980). The two formations are conformable but their contact is sharp (Fig. 2).

Methodology

Sampling and logging of the materials were made in two shallow pits used recently for graphite extraction. Fig. 3 shows stratigraphic logs and sample locations.

Mineralogical studies were based on optical microscopy and X-ray diffraction techniques. The identification of phyllosilicates was based primarily on X-ray diffraction; oriented aggregates of the <20 μm and <2 μm fractions were obtained by sedimentation, and in appropriate cases, they were glycolsolvated and heated at 550 °C for 2 hours. For greater accuracy in spacing determinations, quartz was used as internal standard.

The half height width of the illite 10 Å diffraction peak was measured in the <2 μm fraction using a Phillips 1729 diffractometer, Cu-$K\alpha$ radiation, scanning speed 2°/min, recording speed 20 mm/min and time constant 1 at scale 1 × 10^3 counts per second. The peak widths are shown in 2θ and the boundaries for diagenesis, anchimetamorphism and epimetamorphism are those of Kubler (1967), (2θ = 0.40° and 0.25° respectively). The d(060) spacing of micas and chlorites was measured using a randomly oriented powder of the <2 μm fraction, in the 58° to 63° (2θ) region using the quartz (211) peak as internal standard and at a scanning speed of 0.5°/min.

Carbonaceous matter was isolated by the method of Tagiri (1981); this method eliminates silicate minerals like quartz and micas, whose reflections interfere with the main graphite (002) reflection. The residue was mixed with silicon as internal standard. The analytical conditions were: Cu-$K\alpha$ radiation, at 40 kV and 30 mA, time constant 1 at scale 1 × 10^3 counts per second, scanning speed 1°/min and recording speed 10 mm/min.

As the half height width of the graphite (002) reflection is larger than 0.5° (2θ) in every sample, the correction suggested by Tagiri (1981) was applied in order to correct the diffraction patterns for the Lorentz factor, the polarization factor, the absorption factor and the atomic scattering factor. The 'crystallite size' was calculated using Scherrer's formula: Lc(002) = 91/β, were β is the real width at half height of the gaphite (002) reflection.

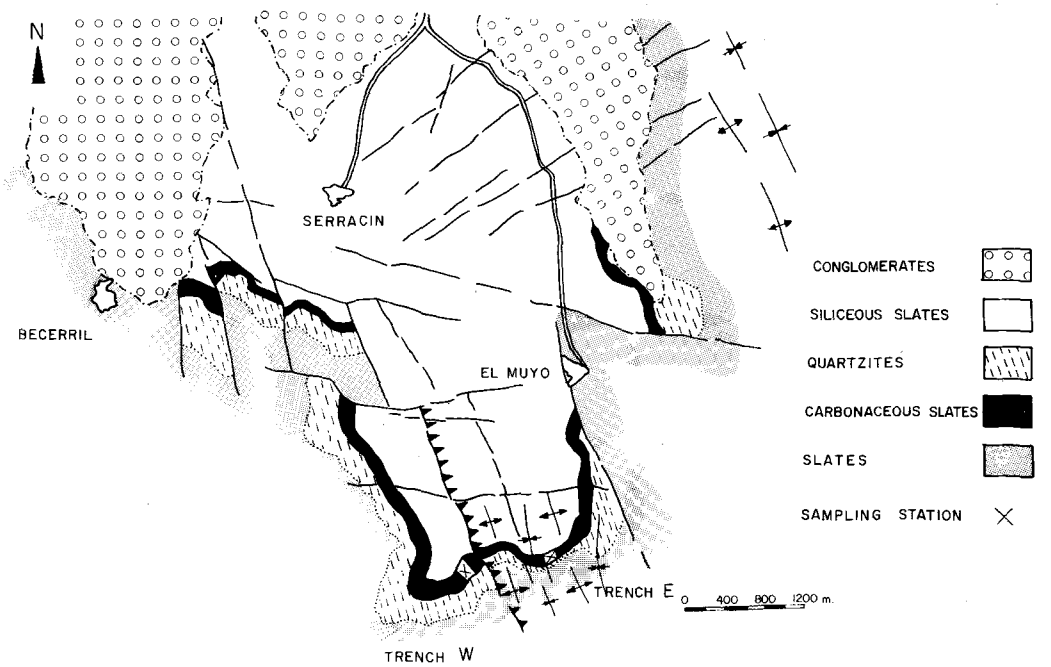

FIG. 2. Detailed map of the Serracin area. Crosses mark the sampling stations.

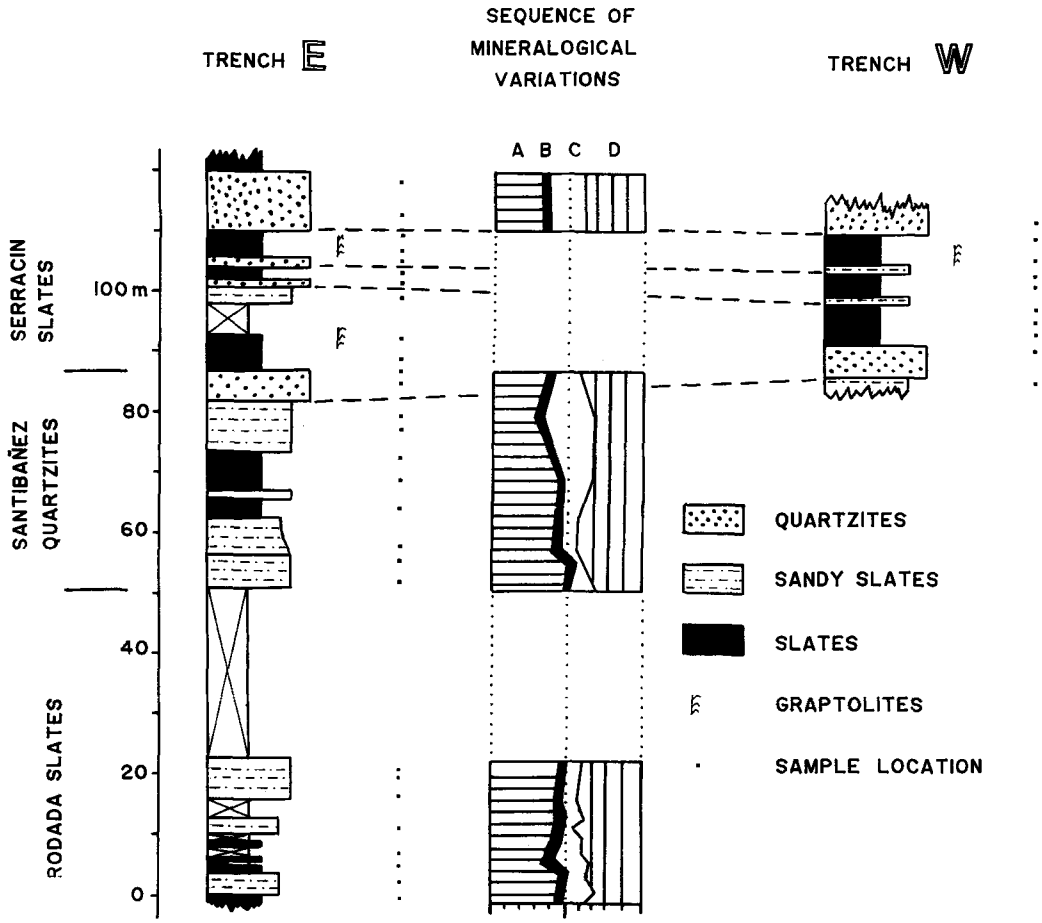

FIG. 3. Logs of two of the sampled trenches. Dots mark the position of the samples. A: Quartz, B: Plagioclase, C: Chlorite, D: Mica.

Results

Mineralogy. Associations and mineral distribution

Two groups of lithologies have been found in the lower Silurian of the study area: (1) 'siliceous slates', with quartz, plagioclase, chlorite and mica, and (2) 'carbonaceous slates', with quartz, plagioclase, graphitized carbonaceous material, mica, and minor amounts of apatite and pyrite.

Siliceous slates

Micas. The micas whose basal spacing remains unchanged at 10 Å following glycolation have been called *illite/muscovite* (Frey, 1987). They are always found in the siliceous slates and define the foliation of the rocks, together with some small quartz crystals. They are dioctahedral micas with $d(060) = 1.500 \pm 0.001$ Å; they correspond to the 2M1 polytype using the 2.58 and 2.80 Å reflections (Maxwell and Hower, 1967).

A value of $(Mg + Fe_{total}) = 0.25$ was calculated from the values obtained for the spacing of the (060) reflection and using the relationship of Guidotti (1984). The Si content was calculated from the values of the $d(002)$ spacing in the muscovites using the relation of Velde (1967), and has a mean value of 6.46 atoms per unit formula.

The values of the half-height width of the illite reflection at 10 Å are represented in Fig. 4 against the ratio of the intensities of the (002) and (001) diffraction peaks. It is obvious that most of the samples recrystallized under epimetamorphic conditions, but close to the anchizone boundary. The $I(002)/I(001)$ values for the micas in the

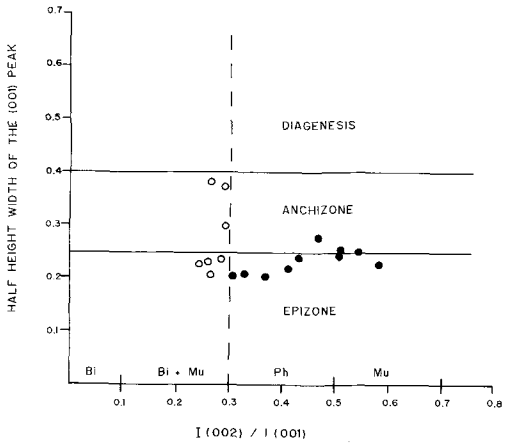

FIG. 4. Relation between width of the (001) peak (in 2θ) and the ratio of intensities of the (002) and (001) peaks for the micas in the Silurian slates of the Serracin Syncline. Limits according to Kubler (1967). Open circles: carbonaceous slates. Solid circles: siliceous slates. *Abbreviations*: Bi = biotite, Bi + Mu = biotite and muscovite, Ph = phengite, Mu = muscovite.

siliceous slates (solid circles in Fig. 4) is higher than 0.3, thus plotting in the phengite field, very common for epizonal micas (Dunoyer de Segonzac, 1970).

Chlorite is only found in the siliceous slates, ranging from 15 to 20%, and never appears in the carbonaceous slates. It shows a grain size smaller than 600 μm, a green colour, no pleochroism, typical low interference colours, and is surrounded by the main schistosity. The fact that $d(060) = 1.549 \pm 0.001$ Å indicates its trioctahedral nature. The polytype corresponds to IIb using the reflections proposed by Moore and Reynolds (1989). The average values of the basal spacing $d(001)$ and the b_0 parameter for 25 chlorites are 14.114 Å and 9.296 Å respectively, as determined by means of X-ray diffraction data. The composition of the octahedral and tetrahedral sites have been calculated from the basic formula $(Mg, Fe, Al)_6 (Si, Al)_4 O_{10} (OH)_8$, using the relations of Kepezhinskas (1965), Albee (1962), and Brindley (1961). From these values the structural formula has been calculated according to Nieto García and Rodríguez Gallego (1982) as:

$$(Mg_{2.20}, Fe_{2.72}, Al_{1.08}) (Si_{2.58}, Al_{1.42}) O_{10} (OH)_8$$

The Fe/(Fe + Mg) ratio and the number of Si^{+4} atoms indicates an Fe-rich composition, corresponding to chamosite (Bayliss, 1975).

Quartz and plagioclase. Quartz occurs in all samples, in a proportion close to 50%. It appears as elongated grains, with a fine to very fine grain size, and is surrounded by the main cleavage primarily defined by the micas. They shown wavy extinction and pressure shadows with mica crystals. Plagioclase is present in these rocks in a proportion lower than 10%. Its composition has been determnined optically as An_{45-50}.

Carbonaceous slates

Micas. The 10 Å micas are the only phyllosilicates in the carbonaceous slates. They are dioctahedral micas and correspond to the 2M1 polytype, similar to those found in the siliceous slates, but with the mean d(060) value slightly different (1.501 Å).

The $I(002)/I(001)$ value for these micas is lower than 0.3 (open circles in Fig. 4) so they are plotted in the biotite + muscovite field. The micas of the siliceous slates are therefore more aluminous than those of the carbonaceous slates (Esquevin, 1969).

Other minerals. The amount of quartz and plagioclase is smaller in the carbonaceous slates, but their optical characteristics are identical. A remarkable feature is a second generation of milky quartz infilling fissures of late-Hercynian age.

Abundant submillimetric pyrite crystals are found in thin laminae parallel to the stratification, and also important is the presence of Ca-phosphate nodules, 2–7 cm wide, in this interval.

Characterization of graphitized carbonaceous matter

We follow the scheme of Landis (1971) for the classification of graphitized organic matter, which proposes several progressive steps from disordered graphite, through graphite d3, d2, d1A, d1, to fully ordered graphite. Other classifications also based upon the increasing crystrallinity of graphite have been proposed (French, 1964; Griffin, 1967).

The chemical composition of representative carbonaceous slates is quite uniform, with carbon contents about 25%, H and N contents about 0.1% and S up to 3.5%.

Fig. 5 shows the X-ray patterns of the carbonaceous material separated from several samples in trenches E and W. They show at least three different graphite types according to the symmetry, intensity and value of the spacing of the (002) reflection. Graphite d3 occurs in the upper part of trench E, graphite d2 in the lower part of the same trench, and graphite d1A in trench W. A different way of representing the evolution of organic matter is the expression of Tagiri (1981):

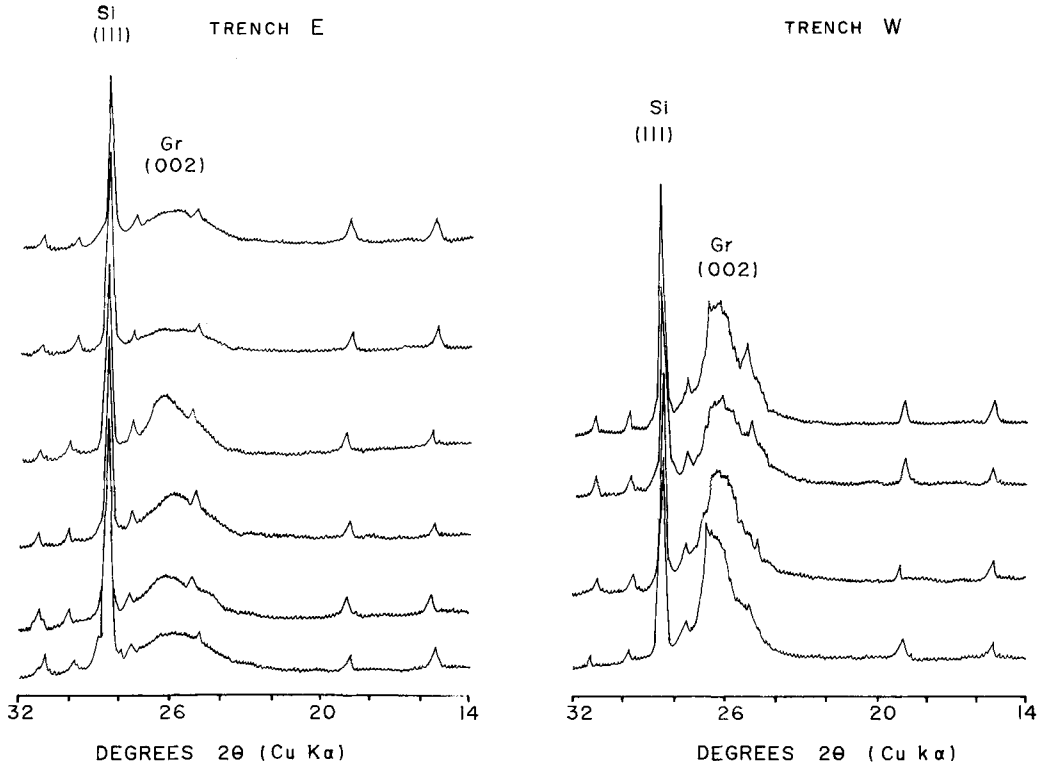

FIG. 5. X-ray diffractograms (from 14° to 32°, 2θ) of the carbonaceous material separated from the Silurian slates. Si: Silicon, Gr: Graphite.

$$G.D. = (d(002) - 3.70)/\log (Lc_{(002)}/1000)*100$$

where G.D. = graphitization degree and $Lc_{(002)}$ = 'crystallite size'. He postulates a hyperbolic relation between $d(002)$ and $Lc_{(002)}$ and thus metamorphic zones are characterized by variation ranges in the graphitization degree. In Fig. 6, the $Lc_{(002)}$ values are plotted against d(002), showing that most of the samples lie in the chlorite zone, close to the anchizone. Samples from trench W show higher values of G.D. and $Lc_{(002)}$.

The measurement of organic matter reflectance in low metamorphic domains causes problems because it is difficult to distinguish the vitrinite particles from other macerals (Teichmüller, 1987). Our samples show a fine intertwining of graphite, quartz and micas and the particles are too small for precise reflectance measurements (Fig. 7). Qualitative estimations show agreement with the XRD data because the highest reflectance values are found in samples from trench W (R_{oMax} = 7%) and the lowest in samples from the upper part of trench E (R_{oMax} = 3%).

Both the XRD and reflectance data show low crystallinity for the carbonaceous matter of the area, but a High-Resolution Transmission Electron Microscopy (HRTEM) study showed areas of high crystallinity with parallel carbon layers very close to low crystallinity areas (Fig. 8), a very similar array to the observations of Buseck and Bo-Jun (1984).

The fact that graphite presents different crystallinities—graphite d3, d2 and d1A–in a small interval of the Silurian slates, indicates that temperature was not the only factor involved. The decrease of 'crystallite size' and graphitization degree in the upper part of trench E can be related to the larger grain size and increased quartz percentage in this interval. Itaya (1981) pointed out the importance of both factors on graphite crystallinity.

The higher graphitization degree on trench W is due to higher shear stresses as clearly shown by the minor deformational structures. Bonijoly *et al.* (1982) and Teichmüller (1987) have observed how shear stress causes a higher crystallinity in graphite because of the local and temporal increase of temperature due to frictional heat.

Therefore, it seems that the crystallinity of carbonaceous matter in the chlorite zone can

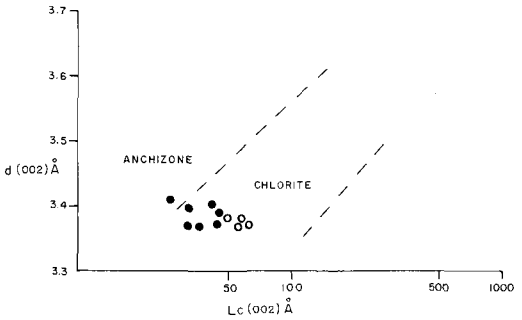

FIG. 6. Relation between $Lc_{(002)}$ and $d(002)$ of the carbonaceous materials. Boundaries according to Pesquera and Velasco (1988).

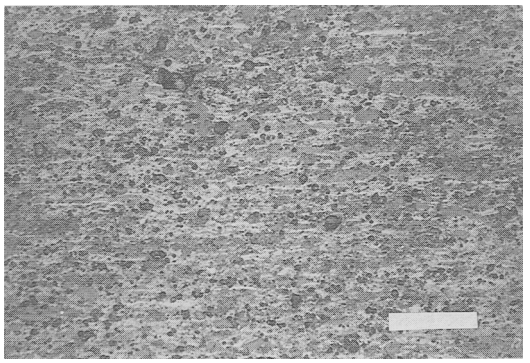

FIG. 7. Intergrowth of mica, quartz (dark coloured grains), and carbonaceous material (light coloured grains). Reflected light, air, Zeiss Axiophot microscope. Bar = 0.5 mm.

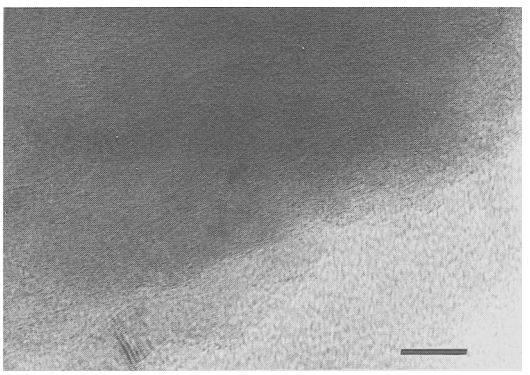

FIG. 8. Graphite layers in a sample from trench W. High Resolution Electron Microscope image. Bar = 200 Å.

change due to factors such as temperature, shear stress and lithology. These conclusions are in agreement with data from Diessel *et al.* (1978), Teichmüller (1987) and Pesquera and Velasco (1988).

Constraints on graphite formation

According to Cathelineau and Nieva (1985) there is a dependance relation between the Al content in the tetrahedral sites of chlorites and the temperature of formation. Cathelineau (1988) modified the original equation by combining the data from different geothermometers.

According to the XRD, EDX and microprobe data the Al^{IV} content in tetrahedral sites averages 1.42 atoms. Using the relation given by Cathelineau and Nieva (1985), the temperature of formation was 300 ± 20 °C, compatible with the mineral assemblages of both types of slates in the area and the anchi-epimetamorphic boundary conditions estimated from the illite crystallinity index. Using the modified equation by Cathelineau (1988), the temperature of formation would be 390 ± 20 °C, too high compared with other independent criteria (Muchez *et al.*, 1991). These results agree with the differences observed between both equations by Hillier and Velde (1991).

On the other hand, Shengelia *et al.* (1979) pointed out that the graphite c_o parameter reflects the maximum temperature reached during the metamorphic period. Using their method, a graph was constructed for the most evolved graphite samples of the sections to obtain a maximum temperature of 310 °C. Although this is only an approximate value, it is in good agreement with the results of the relation proposed by Cathelineau and Nieva (1985); therefore, the value obtained with the second equation should be rejected and we propose a probable temperature of 300 ± 20 °C for the origin of these materials.

Using this temperature and the Si^{4+} content of phengite in the graph of Velde (1967), the formation pressure for these materials can be estimated as about 1.5–2 kbar.

Genetic hypothesis on the origin of the organic matter

The presence of organic-rich sediments is a common feature of the Late Ordovician and Early Silurian sediments of Europe, North Africa and Middle West (Berry and Boucot, 1973; Legget, 1980). If we try to explain the accumulation in the Serracin mineralization, we must recapitulate some of their main characteristics.

The carbonaceous slates show thin parallel lamination as the main internal structure, a good indicator of a quiet environment, below wave action. They overlie quartzites interpreted as open shelf megaripples or sandwaves. The organic carbon content of the mineralized horizon

is very high, up to 25.44%, where black shales have an average content of about 5%. The accumulation rate was very small, about 2.8–4 m per million years.

The vertical changes from the quartzites to the carbonaceous shales is interpreted as the onset of a major transgression at the beginning of the Silurian, following the melting of the large icecap of Central Africa (McKerrow, 1979). The Central System, in the middle of the Iberian microplate was part of an extensive, recently drowned shelf, below wave action, and the oceanic circulation was sluggish; aeration was poor and anoxic conditions were created in this area. The relative isolation from continental sources led to very slow sedimentation allowing for a concentration of organic matter, not diluted by clastic influx; this would be the source of the organic carbon that evolved to graphite during metamorphism.

The abundant submillimetric pyrite crystals are early diagenetic in origin, probably coming from the initial degradation of the organic matter. Planktonic fossils such as Graptolites and Conchostraceae are very well preserved and there is no bioturbation in the organic-rich interval.

The presence of phosphates can be related to important phytoplankton blooms. According to the paleogeographic reconstructions by Paris and Robardet (1990) the Central System was a favourable area for upwelling of deep waters rich in nutrients, with related plankton blooms (Demaison and Moore, 1980). Phytoplankton fixes phosphorous in the photic zone of the ocean; after death, it sinks and most of the present phosphorous is recycled by microbial degradation, but a substantial percentage reaches the ocean floor and is fixed in the sediments to form apatite (Baturin *et al.*, 1972; Veeh and Burnett, 1973).

An alternative to the open-shelf model is a barred basin, where organic carbon-rich sediments can accumulate, but the enormous extension of these facies makes it very improbable.

Conclusions

The Early Silurian materials of the Eastern Spanish Central System contain an organic carbon-rich slates interval with well preserved planktonic fossils, pyrite and phosphate nodules. The interval represents an anoxic period with very slow sedimentation rate, very low energy conditions, no infauna and concentration of organic matter and phosphates.

The carbonaceous slates are composed of quartz, plagioclase (An_{45-50}), graphitized carbonaceous matter, illite/muscovite, pyrite and apatite. The siliceous slates above the carbonaceous interval are composed of quartz, plagioclase (An_{45-50}), phengite, and trioctahedral IIb-type chlorites (chamosite).

The micas show a 'crystallinity index' of 0.25 (2θ), typical of the anchimetamorphism–epimetamorphism boundary. The graphitization degree, 'crystallite size', and *d*(002) of the graphitized organic matter indicate that the materials were metamorphized in the chlorite zone. The metamorphic conditions are estimated about 300 ± 20 °C and 1.5 to 2 kbar.

The XRD study shows different graphite crystallinities (graphite d3, d2 and d1a) in a thin interval and very close outcrops. This is interpreted as the combined effect of regional metamorphism (regional temperature) and local shear stress. To a lesser degree, quartz grain size and impurities have also influenced the crystallinity of graphite.

References

Albee, A. L. (1962) *Am. Mineral.*, **50**, 857–70.

Aparicio, A. and Galán, E. (1980) *Estudios Geológicos.*, **36**, 75–84.

Baturin, G. N., Merkulova, K. J., Chalov, P. I. (1972) *Marine Geol.*, **13**, M37–M41.

Bayliss, P. (1975) *Can. Mineral.*, **13**, 178–80.

Bellido, F., Capote, R., Casquet, C., Fuster, J. M., Navidad, M., Peinado, M., and Villaseca, C. (1981) *Cuadernos de Geología Ibérica*, **7**, 15–52.

Berry, W. B. N. and Boucot, A. J. (1973) *Geol. Soc. Am. Spec. Paper*, **143**, 83 pp.

Bischoff, L. (1974) *Neues Jahrb. Geol. Paläontol. Abh.*, **147**, 218–35.

Bonijoly, M., Oberlin, M., Oberlin, A. (1982) *International Journal of Coal Geology*, **1**, 283–312.

Brindley, G. W., (1961) In *The X-ray Identification and Crystal Structures of Clay Minerals* (G. Brown, ed.) Mineral. Soc. London., 242–96.

Bultynck, P., Soers, E. (1971) *Bull. Inst. R. Sci. Nat. Belg.*, **47**, 1–21.

Buseck, P. R., Bo-Jun, H. (1984) *Geochim. Cosmochim. Acta.*, **49**, 2003–26.

Castaño, J. R. and Sparks, D. M. (1974) *Geol. Soc. America, Spec. Paper*, **153**, 31–52.

Cathelineau, M. (1988) *Clay Minerals*, **23**, 471–85.

—— and Nieva, D. (1985) *Contrib. Mineral. Petrol.*, **91**, 235–44.

Demaison, G. J. and Moore, G. T. (1980) *A.A.P.G. Bull.*, **64**, 1179–209.

Diessel, C. F. K. and Offler, R. (1975) *Neues Jahrb. Mineral.*, Mh., 11–26.

—— Roberts, R. N., and Black, P. M. (1978) *Contrib. Mineral. Petrol.*, **68**, 63–78.

Dunoyer de Segonzac, G. (1970) *Sedimentology*, **15**, 281–346.

Esquevin, J. (1969) *Bull. Centre Rech. Pau-SNPA*, **3**, 147–53.

French, B. M. (1964) *Science*, **146**, 917–8.
Frey, M. (1987) In *Low temperature metamorphism* (M. Frey, ed.). Blackie and Sons, Glasgow, 9–57.
Fuster, J. M. Aparicio, A., Casquet, C., García Cacho, L., Mora, A., and Peinado, M. (1974) *Bol. Geológico y Minero Español*, **85**, (5), 83–88.
González Lodeiro, F. (1983) In *Geología de España. Libro Jubilar J. M. Ríos*, I.G.M.E., Madrid. 408–20.
Griffin, G. M. (1967) *J. Sediment. Petrol*, **37**, 1006–11.
Guidotti, C. V. (1984) In *Micas: Reviews in Mineralogy*, **13**, (S. W. Bailey, ed). Mineral. Soc. America, 357–467.
Hallam, A. and Bradshaw, M. J. (1979) *J. Geol. Soc. London*, **136**, 157–64.
Heckel, P. H. (1977) *A.A.P.G. Bull.*, **61**, 1045–68.
Hillier, S. and Velde, B. (1991) *Clay Minerals*, **26**, 149–68.
Itaya, T. (1981) *Lithos*, **14**, 215–24.
Kepezhinskas, K. B. (1965) *Dokl. Akad. Nauk SSR.*, **164**, 126–9.
Kisch, H. J. (1980) *J. Geol. Soc. London*, **137**, 271–88.
Kubler, B. (1967) In *Etages tectoniques*. A la Baconniére, Neuchátel (Suisse), 105–21.
Landis, C. A. (1971) *Contrib. Mineral. Petrol.*, **30**, 34–45.
Legget, J. K. (1980) *J. Geol. Soc. London*, **137**, 139–56.
Martin, A. K. and Fleming, B. W. (1986) *Can. Soc. Petroleum Geol.*, **2**, 27–44 .
Maxwell, D. T. and Hower, J. (1967) *Am. Mineral.*, **52**, 843–57.
McKerrow, W. S. (1979) *J. Geol. Soc. London*, **136**, 137–45.
Moore, D. M. and Reynolds Jr., R. C. (1989) *X-ray diffraction: identification and analysis of clay minerals*. Oxford University Press. 224–25.
Muchez, P., Boven, J., Bouckaert, J., Leplat, P., Viaene, W., and Wolf, M. (1991) *Neues Jarhb. Geol. Paläont. Abh.*, **182**, 117–31.
Nieto García, F. and Rodríguez Gallego, M. (1982) *Rend. Soc. Ital. Miner. Petrol.*, **38**, 1429–36.
Paris, F. and Robardet, M. (1990) *Tectonophys.*, **177**, 193–213.
Pesquera, A. and Velasco, F. (1988) *Mineral. Mag.*, **52**, 615–25.
Schäfer, G. (1969) *Münster Forsch. Geol. Paläobt.*, **10**, 1–207.
Shengelia, D. M., Akhvledianni, R. A., and Ketskhoveli, D. N. (1979) *Dokl. Akad. Nauk SSSR*, **235**, 1407–9.
Soers, E. (1972) *Studia Geologica* **IV**, 7–94.
Stride, A. H. (1982) *Offshore tidal sands*. Chapman and Hall, New York, 222 pp.
Tagiri, M. (1981) *J. Japan Assoc. Min. Petr. Econ. Geol.*, **76**, 345–52.
Teichmüller, M. (1987) In *Low temperature metamorphism* (M. Frey, ed.). Blackie and Sons. Glasgow, 114–61.
Veeh, H. H., Burnett, W. C. (1973) *Science*, **181**, 844–5.
Velde, B. (1965) *Am. Mineral.*, **50**, 436–49.
—— (1967) *Contrib. Mineral. Petrol.*, **14**, 250–8.

[*Manuscript received 5 August 1991; revised 15 January 1992*]